

DOI:10.1002/ejic.201500759

Crystal Structure and Spectroscopic Investigation of Bromofluoro- and Fluoroiodomethane

Michael Feller,^[a] Karin Lux,^[a] and Andreas Kornath*^[a]

Keywords: Crystal engineering / Noncovalent interactions / σ -Holes / Vibrational spectroscopy / X-ray diffraction

The solid states of bromofluoromethane (BFM) and fluoroiodomethane (FIM) are characterized by X-ray diffraction analysis and by Raman spectroscopy. The single crystals were obtained by crystallization in situ at low temperature. BFM and FIM crystallize in the space group *I2/a* and *Abm2*, respectively. The Raman spectra of both compounds were re-

corded in different aggregation states and at different temperatures. Quantum chemical calculations and the X-ray diffraction data are considered to describe the noncovalent interactions of both compounds in the solid state. These interactions are discussed in the context of the σ -hole concept.

Introduction

The reactivity of dihalogenomethanes (CH_2XF ; X = Cl, Br, I) has been widely investigated because of their ozone-depleting properties (X = Cl)^[1] and their use as fluoromethylating agents (X = Br, I).^[2–5] In the field of crystal engineering, noncovalent interactions of such molecules are of interest.^[6,7] Therefore, intermolecular interactions of several dihalogenomethanes have been studied.^[8–13] Intermolecular interactions are important for the arrangement of structural units, and they play a significant role in determining the physical properties of the compounds.^[14] Hence, investigation of the solid-state structure can improve the potentials derived from physical measurements. Crystallographic data of CH_2XF (X = Cl, Br, I) compounds are only known for CH_2ClF .^[15] This prompted us to investigate the crystal structures of CH_2BrF (BFM) and CH_2FI (FIM) and to undertake a detailed vibrational analyses with the aim of studying the noncovalent interactions.

then repeatedly heated and cooled at a constant rate between 155 and 130 K to obtain a single crystal that was suitable for X-ray diffraction measurements. The X-ray diffraction of BFM was measured at 115 K. In the case of fluoroiodomethane (FIM), the capillary was heated and cooled between 200 and 180 K to obtain a single crystal (m.p. 192 K). The X-ray diffraction analysis of FIM was performed at 173 K.

BFM crystallizes in the monoclinic space group *I2/a* with two symmetrically independent molecules in the asymmetric unit. A view of the molecular structure is shown in Figure 1, and Table 1 contains selected geometric parameters. Carbon atoms C1 and C2 show a slightly distorted tetrahedral coordination due to the different size of the surrounding atoms. The C–Br bond lengths of 1.938(4) and 1.924(4) Å, respectively, are in the region of C–Br bond lengths observed for methyl bromide [1.86(4) Å]^[16] and dibromomethane (1.91 Å).^[17] The C–F bond lengths of 1.377(4) and 1.356(4) Å, respectively, are in the region typical of C–F single bonds.^[18,19]

Results and Discussion

Crystal Structures

Single crystals of BFM were grown in situ in a glass capillary, which was mounted on a diffractometer and cooled by a nitrogen stream at a controlled temperature. The focus of the gas stream was modified by moving the capillary in the vertical direction. The crystallization was monitored visually and by X-ray diffraction. Bromofluoromethane (BFM) froze at ca. 140 K (m.p. 152 K). The capillary was

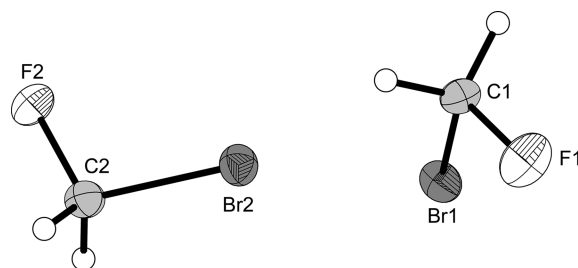


Figure 1. Asymmetric unit of BFM (50% probability displacement ellipsoids).

Figure 2 shows a view of the unit cell of BFM along the *a*- and *b*-axis. The intermolecular $\text{Br}\cdots\text{Br}$ contacts of 3.671(1) and 3.675(3) Å are slightly below the sum of the

[a] Department of Chemistry, Ludwig-Maximilian University of Munich
Butenandtstr. 5-13 (D), 81377 München, Germany
E-mail: andreas.kornath@cup.uni-muenchen.de
<http://www.cup.uni-muenchen.de/ac/kornath/index.php>

Table 1. Selected bond lengths [Å] and bond angles [°] of BFM. Symmetry codes: i: $-x, -0.5 + y, 0.5 - z$; ii: $-x, 0.5 + y, 0.5 - z$.

Bond lengths [Å]				Calcd. ^[a]
C1–F1	1.377(4)	C2–F2	1.356(5)	1.361
C1–Br1	1.938(4)	C2–Br2	1.924(4)	1.933
Bond angles [°]				
F1–C1–Br1	108.1(3)	F2–C2–Br2	109.9(3)	110.5
C1–Br1···Br2i	167.4(1)	C2–Br2···Br2ii	160.1(1)	
C1–Br2···Br2i	122.5(1)	C2–Br2···Br1ii	90.9(2)	

[a] Calculated at the CCSD(T)/TZVPD level of theory with the program package Gaussian 09.^[37]

van der Waals radii (3.70 Å).^[20] One bromine atom (Br1) forms one Br1···Br2i contact, whereas the second bromine atom (Br2) forms contacts with two further bromine atoms (Br2i and Br2ii) (Figure 2). Two of the overall four C–Br···Br angles are closer to a right angle [90.9(1)° and 122.5(1)°], whereas the other two C–Br···Br angles with 160.1(1)° and 167.4(1)° are rather close to 180°. Such contacts are also observed in the crystal structures of methyl bromide^[16] and dibromomethane,^[17] and they are indicative of a noncovalent bonding type (see below).^[21,22]

FIM crystallizes in the orthorhombic space group *Abm2* with four units per unit cell. A view of the molecular structure is shown in Figure 3, and Table 2 contains selected geometric parameters. The fluorine atom is disordered over two positions with an occupancy of 50%. The C–I bond length of 2.132(12) Å is in the region of C–I bond lengths observed for methyl iodide [2.13(6) Å]^[16] and diiodomethane

(2.12 Å).^[17] The C–F bond length of 1.380(18) Å is in the region typical of C–F single bonds.^[18,19]

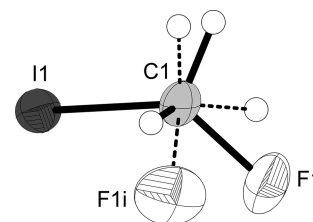


Figure 3. Asymmetric unit of FIM (50% probability displacement ellipsoids). Symmetry code: i: $x, 0.5 - y, z$.

Table 2. Selected bond lengths [Å] and bond angles [°] of FIM.

Bond lengths [Å]		
C1–F1	1.380(17)	Calcd. ^[a]
C1–I1	2.132(12)	2.133
Bond angles [°]		
F1–C1–I1	109.7(11)	110.7
C1–I1···I1ii	180.0(3)	
C1–I1···I1i	92.0(3)	

[a] Calculated at the CCSD(T)/TZVPD level of theory with the program package Gaussian 09.^[37]

Figure 4 shows a view of the unit cell of FIM along the *b*-axis. The intermolecular I···I contacts of 3.938(1) Å are slightly below the sum of the van der Waals radii (3.96 Å).^[20] Each iodine atom is in contact with two further iodine atoms. The C–I···I angles are 92.0(3)° and 180.0(3)°.

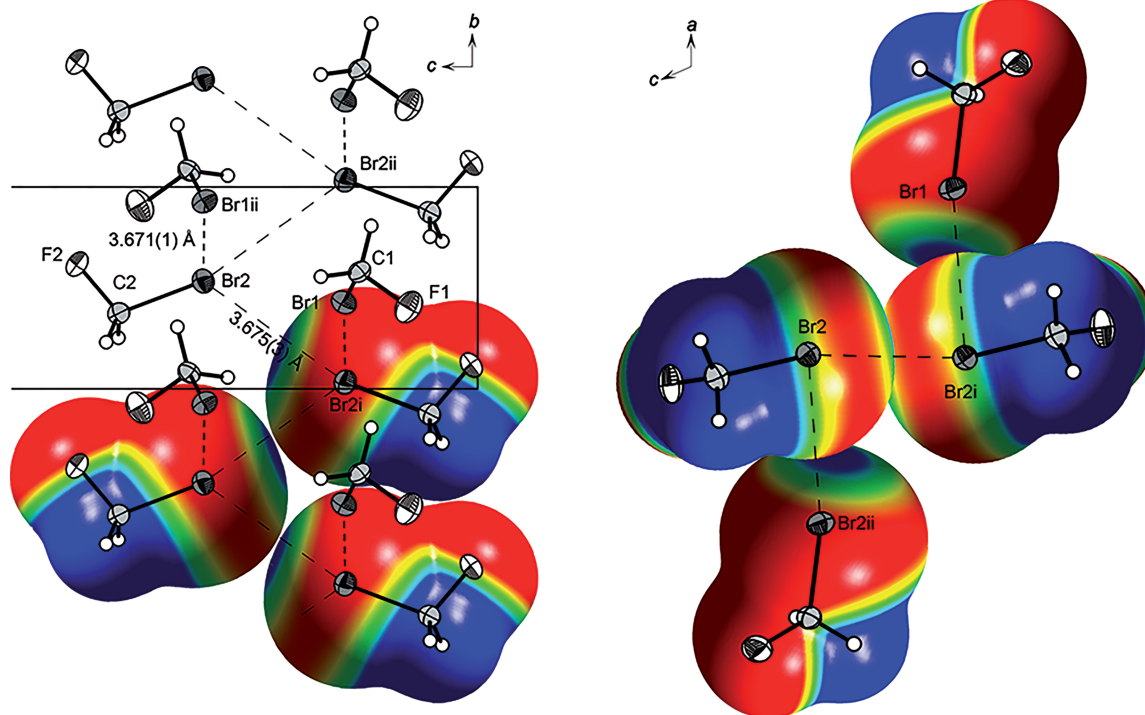


Figure 2. View of the unit cell along the *a*-axis (left) and *b*-axis (right); Br···Br contacts are indicated as dashed lines between the molecules represented as atomic thermal ellipsoids (50% probability displacement ellipsoids), superimposed onto the molecular isosurface with mapped electrostatic potential as a color scale ranging from -0.01 a.u. (red) and 0.01 a.u. (blue); isoval. = 0.0004; symmetry codes: i: $-x, -0.5 + y, 0.5 - z$; ii: $-x, 0.5 + y, 0.5 - z$. Asymmetric unit of BFM (50% probability displacement ellipsoids).

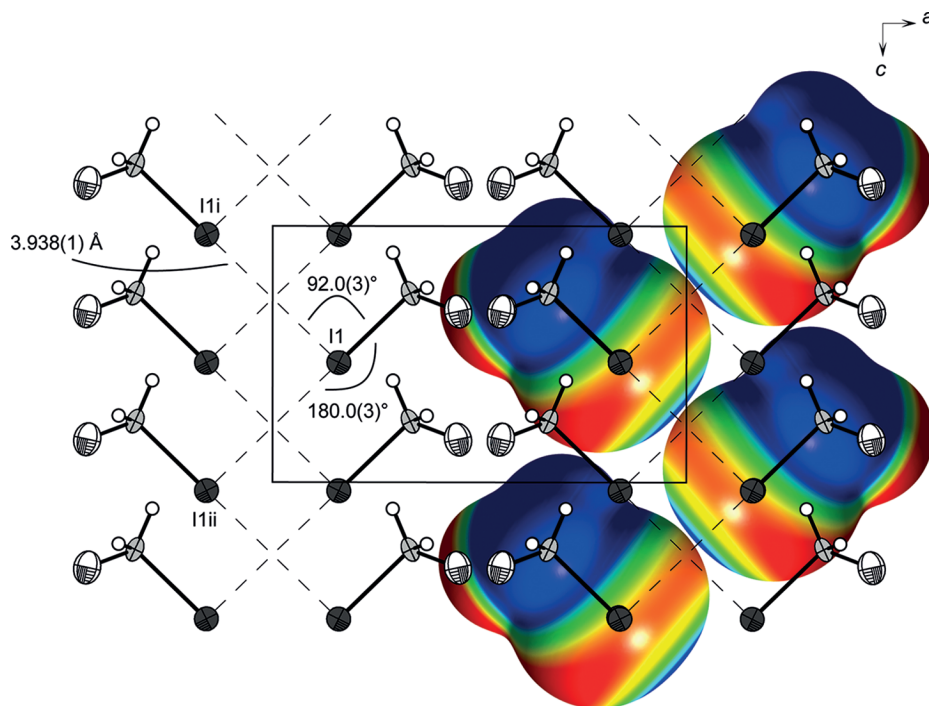


Figure 4. View of the unit cell along the *b*-axis; I...I contacts are indicated by dashed lines between the molecules represented as atomic thermal ellipsoids (50% probability displacement ellipsoids), superimposed onto the molecular isosurface with mapped electrostatic potential as a color scale ranging from -0.01 a.u. (red) and 0.01 a.u. (blue); isoval. = 0.0004 ; symmetry codes: i: $-x, 0.5 - y, -0.5 + z$; ii: $-x, 0.5 - y, 0.5 + z$.

Such I...I interactions are also observed in the solid-state structures of methyl iodide^[16] and diiodomethane.^[17]

Theoretical and experimental studies have shown that dispersion and polarization participate in the molecular interactions of dihalogenomethanes.^[8] However, the halogen interactions are believed to be mainly controlled by electrostatics^[23] and are Coulombic in nature.^[24] The superimposed electrostatic potential surfaces of BFM (Figure 2) and FIM (Figure 4) show anisotropic distributions of the electron densities around the halogen atoms. The negative potential rings of one halogen atom and positive electrostatic end caps of a neighboring halogen atom are directed towards each other. This characteristic is referred to as the σ -hole.^[21,22] Given that heavier atoms are more polarizable, the anisotropic distribution of the electron density around a halogen atom increases in the order $\text{Cl} < \text{Br} < \text{I}$ (Figure 5).^[8]

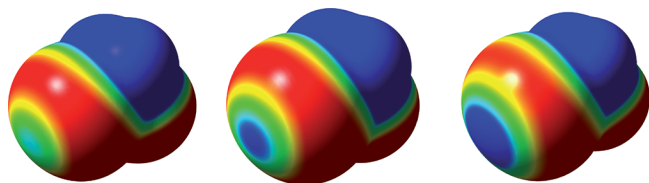


Figure 5. Molecular 0.0004 bohr^{-3} 3D isosurfaces with mapped electrostatic potential as a color scale ranging from -0.01 a.u. (red) to 0.01 a.u. (blue). The electrostatic potential isosurfaces have been calculated for the molecules CH_2ClF (left), CH_2BrF (middle), and CH_2IF (right).

The interactions of the halogen atoms are also characterized by the angle $\theta_i = \text{C}\cdots\text{X}_i\cdots\text{X}_{i+1}$. Two different types of interactions have been described previously.^[6] If the angle θ_i is equal to θ_{i+1} the interactions are believed to be a result of close packing. At an angle of $\theta_i = 180^\circ$ and $\theta_{i+1} = 90^\circ$ the interactions are considered to result from polarization of the adjacent atoms. The angles θ_i and θ_{i+1} in the crystal structures of BFM and FIM are close to 180° and 90° , respectively. This supports the assumption that σ -holes play an important role in determining the characteristics of these molecules. It should be noted that the structures of several halogenomethanes CH_3X ($\text{X} = \text{Cl}, \text{Br}, \text{I}$) involve hydrogen bonds that are in competition with halogen...halogen interactions.^[8] In the case of CH_2FX ($\text{X} = \text{Cl}, \text{Br}, \text{I}$) compounds, $\text{F}\cdots\text{H}$ contacts shorter than the sum of the van der Waals radii are found (Table 3), which also indicate a competition between $\text{F}\cdots\text{H}$ and $\text{X}\cdots\text{X}$ interactions. However, $\text{X}\cdots\text{X}$ distances below the sum of the van der Waals radii are only observed for BFM and FIM (Table 3).

Table 3. Intermolecular distances of FIM, BFM, and CFM (chloroform) less than the sum of the van der Waals radii.

	FIM	BFM	CFM ^[15]
$\text{X}\cdots\text{X}$ [Å]	3.938(1)	3.671(1), 3.675(3)	3.525(9)
$\text{F}\cdots\text{H}$ [Å]	2.446(18)	2.576(37)	2.511(13)

Raman Spectroscopy

The solid state of BFM and FIM was also studied by vibrational spectroscopy. The Raman spectra shown in Fig-

ure 6 were recorded at 77 and 10 K, and they are compared with those of the liquid state. The vibrational data together with quantum chemically calculated frequencies are listed in Tables 4 and 5. For the assignment of the vibration, an ideal C_s symmetry was considered for both molecules. Consequently, nine fundamental vibrations ($6 A' + 3 A''$) are expected. The assignment of the vibrations is based on the Cartesian displacement coordinates of the theoretical calculated frequencies. The solid-state Raman spectra show a band splitting that is caused by the crystal fields of the compounds. The Raman lines at 3072 cm^{-1} (BFM) and 3060 cm^{-1} (FIM) are assigned to the antisymmetric C–H stretching vibration, and the Raman lines at 2996 cm^{-1} (BFM) and 2980 cm^{-1} (FIM) are assigned to the symmetric C–H stretching vibration. In the case of BFM, the band shape changes significantly between 77 and 10 K. This may indicate a phase transition in this temperature region. The description of the physical meaning of the CH_2 bending modes below 1400 cm^{-1} is rather tentative, and it should be noted that these vibrations contain the H–C–F and H–C–X bending modes. The C–F stretching vibrations appear in their typical region around 1340 cm^{-1} .^[25] The C–X (X = Br, I) stretching vibrations occur at 638 and 564 cm^{-1} , respectively. In the case of BFM, the C–Br stretching mode and the overtone of the Br–C–F bending mode leads to a Fermi resonance doublet, which is well resolved in the solid state.^[26–28]

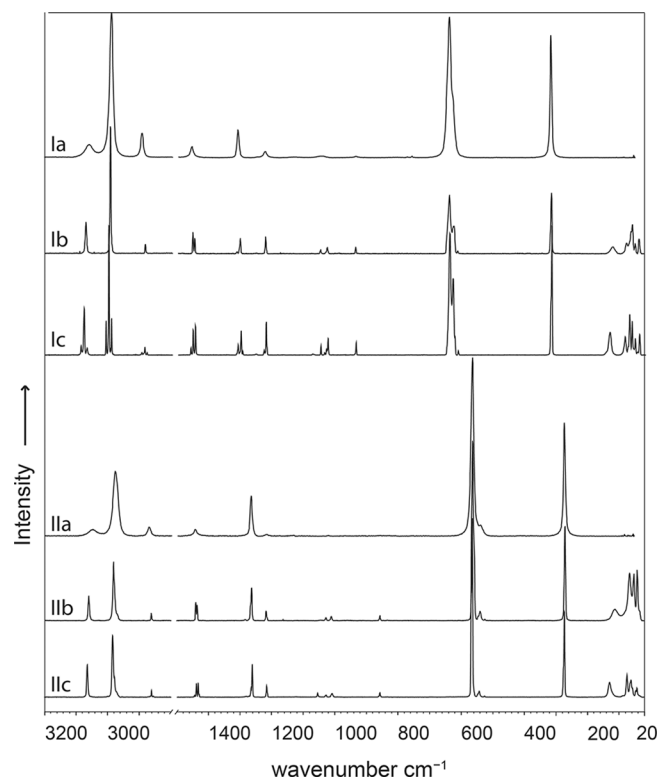


Figure 6. Raman spectra of liquid (Ia, IIa) and solid BFM (top) and FIM (bottom). The Raman spectra of the solid compounds were recorded at 77 K (Ib, IIb) and 10 K (Ic, IIc), respectively.

Table 4. Vibrational modes and assignments of BFM.

Liquid	Solid (77 K)	Solid (10 K)	Calcd. ^[a]	Assignm.
3060 (9)	3072 (25)	3087 (7) 3077 (36) 3068 (6) 3008 (27)	3067	$\nu_7(A'')$ $\nu_{\text{as}}(\text{CH}_2)$
2990 (100)	2996 (100)	2999 (100) 2991 (5) 2896 (2)	2989	$\nu_1(A')$ $\nu_{\text{s}}(\text{CH}_2)$
2894 (17)	2886 (7)	2886 (6) 2880 (2) 1460 (5)		$2\nu_2(A')$ $\delta(\text{CH}_2)$
1456 (8)	1452 (17) 1447 (12)	1454 (16) 1446 (19) 1311 (7)	1459	$\nu_2(A')$ $\delta(\text{CH}_2)$
1310 (20)	1302 (12)	1302 (16) 1297 (3) 1229 (3)	1313	$\nu_3(A')$ $\omega(\text{CH}_2)$
1224 (4) 1048 (1)	1222 (13) 1048 (3)	1222 (22) 1048 (6) 1037 (2) 1031 (4)	1222 1064	$\nu_8(A'')$ $\tau(\text{CH}_2)$ $\nu_4(A')$ $\nu(\text{CF})$
936 (1) 638	1026 (5) 936 (5) 638 (46) 624 (22)	1026 (11) 937 (8) 640 (80) 629 (50) 613 (3)	923 635	$\nu_9(A'')$ $\rho(\text{CH}_2)$ $\nu_5(A')$ $\nu(\text{CBr})$ ^[b] $2\nu_6$ ^[b]
317 (8)	315 (48) 121 (5) 76 (8) 62 (18) 59 (9) 50 (8) 36 (12)	317 (85) 133 (15) 84 (12) 70 (27) 63 (23) 52 (11) 39 (13)	307	$\nu_6(A')$ $\delta(\text{CBrF})$

[a] Calculated at the CCSD(T)/TZVPD level of theory with the program package Gaussian 09.^[37] Frequencies are scaled with an empirical factor of 0.9655. Raman activity is stated on a scale of 1 to 100. Calculated Raman intensities in $\text{\AA}^4\mu^{-1}$. [b] Fermi doublet of these two vibrations.

Table 5. Vibrational modes and assignment of FIM.

Liquid	Solid (77 K)	Solid (10 K)	Calcd. ^[a]	Assignm.
3048 (4) 2978 (36)	3060 (14) 2985 (28) 2985 (28)	3065 (15) 2985 (28) 2978 (9)	3061 2981	$\nu_7(A'')$ $\nu_{\text{as}}(\text{CH}_2)$ $\nu_1(A')$ $\nu_{\text{s}}(\text{CH}_2)$
2872 (64)	2862 (4)	2862 (3) 2855 (1) 1444(1)		$2\nu_2(A')$
1445 (4)	1440 (10) 1435 (9)	1439 (8) 1434 (8)	1443	$\nu_2(A')$ $\delta(\text{CH}_2)$
1268 (23)	1263 (18) 1217 (6) 1028 (2) 1011 (3) 857 (3)	1266 (5) 1216 (6) 1028 (1) 1009 (2) 857 (2)	1271 1209 1043	$\nu_3(A')$ $\omega(\text{CH}_2)$ $\nu_8(A'')$ $\tau(\text{CH}_2)$ $\nu_4(A')$ $\nu(\text{CF})$
564 (100) 539 (6)	564 (100) 540 (5) 271 (52) 112 (6) 67 (26)	564 (100) 543 (3) 273 (48) 130 (8) 74 (12) 61 (10)	848 568 262	$\nu_9(A'')$ $\rho(\text{CH}_2)$ $\nu_5(A')$ $\nu(\text{CI})$ $2\nu_6$ $\nu_6(A')$ (CIF)
	53 (26) 43 (28)	57 (6) 46 (4) 43 (5)		

[a] Calculated at the CCSD(T)/TZVPD level of theory with the program package Gaussian 09.^[37] Frequencies are scaled with an empirical factor of 0.9655. Raman activity is stated on a scale of 1 to 100. Calculated Raman intensities in $\text{\AA}^4\mu^{-1}$.

Conclusions

The solid states of BFM and FIM were characterized by X-ray diffraction analysis and by Raman spectroscopy. The crystal structures of BFM and FIM revealed halogen distances that are shorter than the sum of the van der Waals radii. The calculation of electrostatic potentials of CFM, BFM, and FIM show an increasing anisotropic distribution of the electron density with increasing size of the halogen atom. Only in the case of FIM is a perpendicular arrangement of the halogen atoms observed, whereas BFM and FIM reveal σ -holes. This is in accordance with the halogen interactions in the crystal packing, which increases in the series $\text{Cl} < \text{Br} < \text{I}$. The Raman spectra of solid BFM indicate a phase transition between 77 and 10 K.

Experimental Section

Apparatus and Materials: Synthesis and sample handling were performed by employing standard Schlenk techniques and a stainless-steel vacuum line. The Raman spectra of liquid and solid BFM and FIM were recorded using the regular entrance slit of a Jobin Yvon ISA T64000 spectrometer and an argon ion laser (Stabilite 2017, Spectra Physics, $\lambda = 514.5 \text{ nm}$) as irradiation source. The Raman spectra at 77 K were recorded using a low-temperature cell. For the measurements at 10 K, our Raman matrix isolation spectroscopy apparatus was used.^[29] The low-temperature X-ray diffraction of BFM and IFM was performed with an Oxford XCal-

ibur3 diffractometer equipped with a Spellman generator (voltage 50 kV, current 40 mA) and a KappaCCD detector, operating with Mo- K_{α} radiation ($\lambda = 0.7107 \text{ \AA}$). Data collections at 173 K were performed using the CrysAlis CCD software,^[30] the data reductions were carried out using the CrysAlis RED software.^[31] The solution and refinement of the structure was performed with the programs SHELXS^[32] and SHELXL-97^[33] implemented in the WinGX software package^[34] and finally checked with the PLATON software.^[35] Selected data and parameters of the X-ray analysis are given in Table 6. CCDC-1004462 (BFM) and 1004463 (FIM) contain the supplementary crystallographic data. These data can be obtained free of charge from The Cambridge Crystallographic Data Centre via www.ccdc.cam.ac.uk/data_request/cif.

Synthesis of Bromofluoromethane and Fluoroiodomethane: The synthesis of the compounds was performed as reported previously.^[36] An excess of silver nitrate (55 mmol, 9.4 g) was added to an aqueous solution of sodium fluoroacetate (50 mmol, 5 g). The almost insoluble silver monofluoroacetate was filtered and then dried in vacuo over phosphoric oxide (7.9 g, 42.5 mmol, yield 85%). The silver salt (4 g, 21 mmol) was heated in a sealed tube with bromine (4.0 g, 25 mmol) from 50 to 120 °C during 6 h. The crude product was purified by microdistillation to give BFM (1.4 g, 13 mmol). For the synthesis of FIM, silver monofluoroacetate (4 g, 21 mmol) and iodine (2.7 g, 21 mmol) were premixed and slowly heated to 160 °C. The crude product was continuously removed by condensation into a trap cooled with dry ice. The crude product was purified by microdistillation to give FIM (1.3 g, 8 mmol).

Theoretical Calculations: Quantum chemical calculations were performed with the Gaussian 09 program package^[37] using the CCSD-

Table 6. X-ray data and parameters for BFM and FIM.

	BFM	FIM
Empirical formula	CH ₂ BrF	CH ₂ FI
M_r [g mol ⁻¹]	112.94	159.93
Cryst. size [mm]	0.25 × 0.12 × 0.1	0.2 × 0.08 × 0.05
Crystal system	monoclinic	orthorhombic
Space group	<i>I2/a</i>	<i>Abm2</i>
<i>a</i> [Å]	16.720(3)	8.8664(10)
<i>b</i> [Å]	4.2321(6)	7.0889(7)
<i>c</i> [Å]	18.677(4)	5.4675(5)
α [°]	90	90
β [°]	113.56(2)	90
γ [°]	90	90
<i>V</i> [Å ³]	1211.4(4)	343.65(6)
<i>Z</i>	16	4
ρ_{calcd} [g cm ⁻³]	2.477	3.091
μ [mm ⁻¹]	13.292	9.072
$\lambda(\text{Mo-}K_{\alpha})$ [Å]	0.71073	0.71073
<i>F</i> (000)	832	280
<i>T</i> [K]	115(2)	173(2)
<i>hkl</i> range	-20→14; -5→4; -17→23	-10→11; -9→9; -7→7
Refl. measured	2856	1586
Refl. unique	1192	428
<i>R</i> _{int}	0.0325	0.0801
Parameters	55	23
<i>R</i> (<i>F</i>)/ <i>wR</i> (<i>F</i> ²) ^[a] (all reflexions)	0.0396/0.0518	0.0415/0.1040
Weighting scheme ^[b]	0.0134/0.0	0.0678/0.0
<i>S</i> (GoF) ^[c]	0.921	1.088
Residual density [e Å ⁻³]	0.523/-0.365	0.941/-0.760
Device type	Oxford XCalibur	Oxford XCalibur
Solution/refinement	SHELXS-97/SHELXL-97	SHELXS-97/SHELXL-97
CCDC	1004462	1004463

[a] $R_1 = \Sigma |F_o| - |F_c| / \Sigma |F_o|$, [b] $wR_2 = \{\Sigma [w(F_o^2 - F_c^2)^2] / \Sigma [w(F_o^2)]\}^{1/2}$; $w = [\sigma_c^2(F_o^2) + (xP)^2 + yP]^{-1}$; $P = (F_o^2 + 2F_c^2)/3$. [c] GoF = $\{\Sigma [w(F_o^2 - F_c^2)^2] / (n - p)\}^{1/2}$ (n = number of reflections; p = total number of parameters).

T coupled cluster method and the Def2-TZVPD basis. The method was used for the theoretical calculations referring to reported data.^[38] The triple excitations were calculated noniteratively. Frequencies of the fundamentals were calculated at the fully optimized structure. The frequencies were scaled by an empirical factor of 0.9655. For the calculation of the electrostatic potentials, geometry parameters from the crystallographic data were used. The 0.0004 bohr⁻³ 3D isosurface was mapped with the electrostatic potential as a color scale ranging from -0.01 to 0.01 a.u. (-6.3 to 6.3 kcal/mol).

Acknowledgments

Financial support of this work by the Ludwig-Maximilian University of Munich (LMU) and the Deutsche Forschungsgemeinschaft (DFG) is gratefully acknowledged.

- [1] R. J. Cicerone, R. S. Stolarski, S. Walters, *Science* **1974**, *185*, 1165–1167.
- [2] K. J. Jadav, S. Kambhampati, T. R. Chitturi, R. Thennati, Patent Application, US20050256325A1, **2003**.
- [3] D. H. R. Barton, R. H. Hesse, M. M. Pechet, T. J. Tewson, *J. Chem. Soc. Perkin Trans. 1* **1973**, 2365–2370.
- [4] E. P. T. Leitao, C. R. Turner, Patent Application, US20130225844A1, **2011**.
- [5] P. J. Joseph, W. D. Sherod, Patent Application, WO2003013427A2, **2003**.
- [6] P. Politzer, J. S. Murray, *ChemPhysChem* **2013**, *14*, 278–294.
- [7] P. Politzer, P. Lane, M. C. Concha, Y. Ma, J. S. Murray, *J. Mol. Model.* **2007**, *13*, 305–311.
- [8] M. Esrafil, M. Vakili, M. Solimannejad, *J. Mol. Model.* **2014**, *20*, 1–6.
- [9] F. F. Awwadi, R. D. Willett, K. A. Peterson, B. Twamley, *Chem. Eur. J.* **2006**, *12*, 8952–8960.
- [10] F. F. Awwadi, R. D. Willett, K. A. Peterson, B. Twamley, *J. Phys. Chem. A* **2007**, *111*, 2319–2328.
- [11] M. Podsiadło, A. Katrusiak, *Acta Crystallogr., Sect. B* **2007**, *63*, 903–911.
- [12] M. Podsiadło, A. Katrusiak, *CrystEngComm* **2008**, *10*, 1436–1442.
- [13] M. Podsiadło, A. Katrusiak, *CrystEngComm* **2009**, *11*, 1391–1395.
- [14] H. M. Yamamoto, J.-I. Yamaura, R. Kato, *J. Am. Chem. Soc.* **1998**, *120*, 5905–5913.
- [15] O. S. Binbrek, B. H. Torrie, I. P. Swainson, *Acta Crystallogr., Sect. C: Cryst. Struct. Commun.* **2002**, *58*, o672–o674.
- [16] T. Kawaguchi, M. Hijikigawa, Y. Hayafuji, M. Ikeda, R. Fukushima, Y. Tomiie, *Bull. Chem. Soc. Jpn.* **1973**, *46*, 53–56.
- [17] T. Kawaguchi, A. Wakabayashi, M. Matsumoto, T. Takeuchi, T. Watanabe, *Bull. Chem. Soc. Jpn.* **1973**, *46*, 57–61.
- [18] A. F. Holleman, E. Wiberg, *Lehrbuch der Anorganischen Chemie* (Ed.: N. Wiberg), 102. ed., de Gruyter, Berlin **2007**, pp. 2006.
- [19] O. S. Binbrek, B. H. Torrie, I. P. Swainson, *Acta Crystallogr., Sect. C* **2002**, *58*, o672–o674.
- [20] A. Bondi, *J. Phys. Chem.* **1964**, *68*, 441–451.
- [21] P. Politzer, J. S. Murray, T. Clark, *Phys. Chem. Chem. Phys.* **2013**, *15*, 11178–11189.
- [22] T. Clark, *WIREs Comput. Mol. Sci.* **2013**, *3*, 13–20.
- [23] J. P. M. Lommerse, A. J. Stone, R. Taylor, F. H. Allen, *J. Am. Chem. Soc.* **1996**, *118*, 3108–3116.
- [24] P. Politzer, J. S. Murray, T. Clark, *Top. Curr. Chem.* **2015**, *358*, 19–42.
- [25] T. Soltner, N. R. Goetz, A. Kornath, *Eur. J. Inorg. Chem.* **2011**, 3076–3081.
- [26] A. Baldacci, A. Baldan, A. Gambi, P. Stoppa, *J. Mol. Struct.* **2000**, *517–518*, 197–208.
- [27] K. S. Pitzer, E. Gelles, *J. Chem. Phys.* **1953**, *21*, 855–858.
- [28] M.-L. Delwaille, F. François, *J. Phys. Radium* **1946**, *7*, 15–32.
- [29] A. Kornath, *J. Raman Spectrosc.* **1997**, *28*, 9–14.
- [30] *CrysAlisCCD*, version 1.171.36.24 (release 03-12-2012 CrysAlis 171.NET), Oxford Diffraction Ltd. **2012**.
- [31] *CrysAlisRED*, version 1.171.36.24 (release 03-12-2012 CrysAlis 171.NET), Oxford Diffraction Ltd. **2012**.
- [32] G. M. Sheldrick, *SHELXS-97, Program for Crystal Structure Solution*, University of Göttingen, Germany, **1997**.
- [33] G. M. Sheldrick, *SHELXL-97, Programm for the Refinement of Crystal Structures*, University of Göttingen, Germany, **1997**.
- [34] L. J. Farrugia, *J. Appl. Crystallogr.* **1999**, *32*, 837–838.
- [35] A. L. Spek, *PLATON, A Multipurpose Crystallographic Tool*, Utrecht University, Utrecht, The Netherlands, **1999**.
- [36] R. N. Haszeldine, *J. Chem. Soc.* **1952**, 4259–4268.
- [37] M. J. Frisch, G. W. Trucks, H. B. Schlegel, G. E. Scuseria, M. A. Robb, J. R. Cheeseman, G. Scalmani, V. Barone, B. Mennucci, G. A. Petersson, H. Nakatsuji, M. Caricato, X. Li, H. P. Hratchian, A. F. Izmaylov, J. Bloino, G. Zheng, J. L. Sonnenberg, M. Hada, M. Ehara, K. Toyota, R. Fukuda, J. Hasegawa, M. Ishida, T. Nakajima, Y. Honda, O. Kitao, H. Nakai, T. Vreven, J. A. Montgomery Jr., J. E. Peralta, F. Ogliaro, M. Bearpark, J. J. Heyd, E. Brothers, K. N. Kudin, V. N. Staroverov, R. Kobayashi, J. Normand, K. Raghavachari, A. Rendell, J. C. Burant, S. S. Iyengar, J. Tomasi, M. Cossi, N. Rega, J. M. Millam, M. Klene, J. E. Knox, J. B. Cross, V. Bakken, C. Adamo, J. Jaramillo, R. Gomperts, R. E. Stratmann, O. Yazyev, A. J. Austin, R. Cammi, C. Pomelli, J. W. Ochterski, R. L. Martin, K. Morokuma, V. G. Zakrzewski, G. A. Voth, P. Salvador, J. J. Dannenberg, S. Dapprich, A. D. Daniels, Ö. Farkas, J. B. Foresman, J. V. Ortiz, J. Cioslowski, D. J. Fox, *Gaussian 09*, revision A.02, Gaussian, Inc., Wallingford, CT, **2009**.
- [38] A. Gambi, *Mol. Phys.* **2007**, *105*, 2829–2837.

Received: July 10, 2015

Published Online: October 22, 2015